Supporting Information for:

Bridging the immiscibility of an all-fluoride fire extinguishant with highly-fluorinated electrolyte toward safe sodium metal batteries

Xueying Zheng,[1] Zhenyi Gu,[2] Xuyang Liu,[1] Zhongqiang Wang,[1] Jiayun Wen,[1] Xinglong Wu,[2] Wei Luo,[1,*] Yunhui Huang[1,*]

[1]Institute of New Energy for Vehicles, School of Materials Science and Engineering, Tongji University, Shanghai 201804, China

E-mail: weiluo@tongji.edu.cn; huangyh@tongji.edu.cn

[2]Key Laboratory for UV Light-Emitting Materials and Technology of Ministry of Education, National and Local United Engineering Laboratory for Power Batteries, Faculty of Chemistry, Northeast Normal University, Changchun, Jilin 130024, China

* Corresponding authors

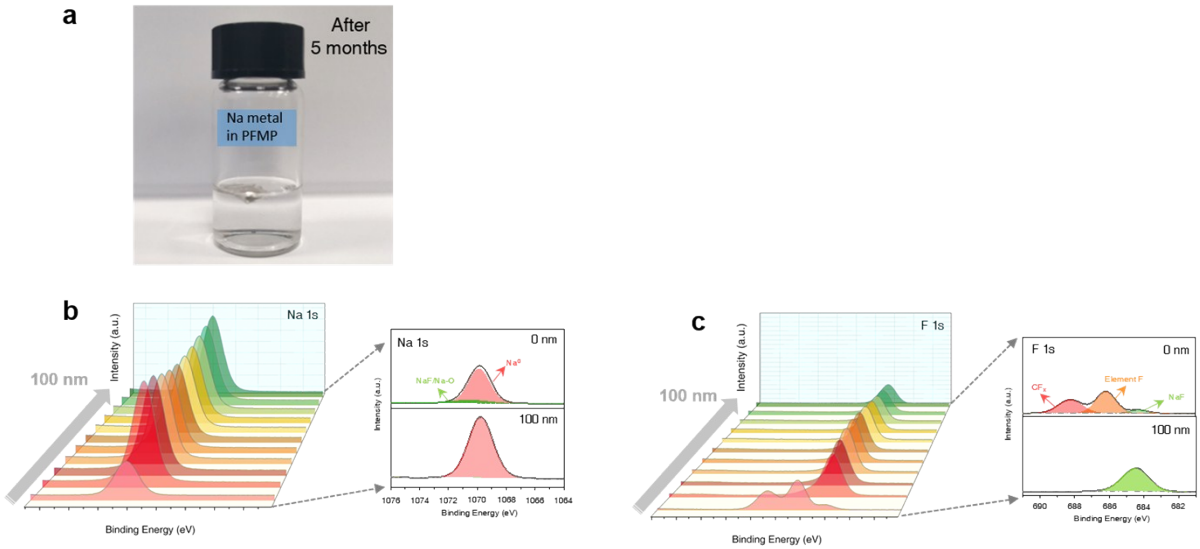

Figure S1. (**a**) Optical photo of the metallic Na after immersing in PFMP for 4 months. (**b**) Na 1s and (**c**) F 1s XPS spectra of the metallic Na after 4 months storage in PFMP with depth profiles.

The piece of metallic Na still shows its metallic cluster after immersing in PFMP for up to 4 months, when harvested for in-depth X-ray photoelectron spectroscopy (XPS) analysis, only minor NaF and CF_x accumulation was detected, along with strong peak of Na^0, suggesting that the Na metal was only the superior physicochemical stability of PFMP toward Na metal.

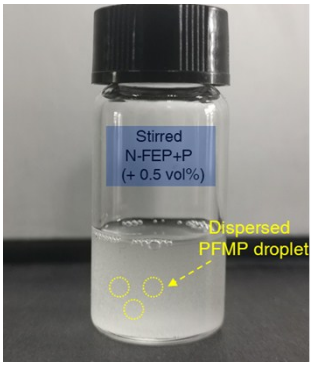

Figure S2. Optical photo of the dispersed PFMP (5 vol%) in the electrolyte of N-FEP after violent stirring. By violent magnetic stirring, the PFMP was able to uniformly disperse in the N-FEP electrolyte, forming a temporary suspension and was immediately used for flammability test.

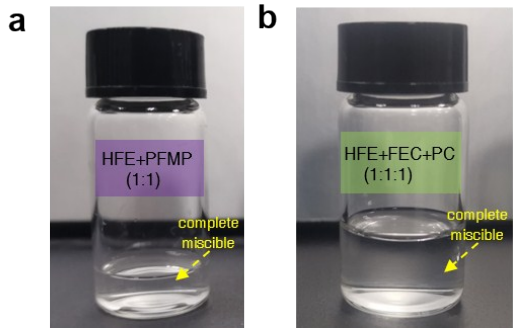

Figure S3. Optical photo showing the complete miscibility of HFE with (**a**) PFMP in a volumetric ratio of 1:1 vol% and with (**b**) FEC/PC in a volumetric ratio of 1:1:1 vol%.

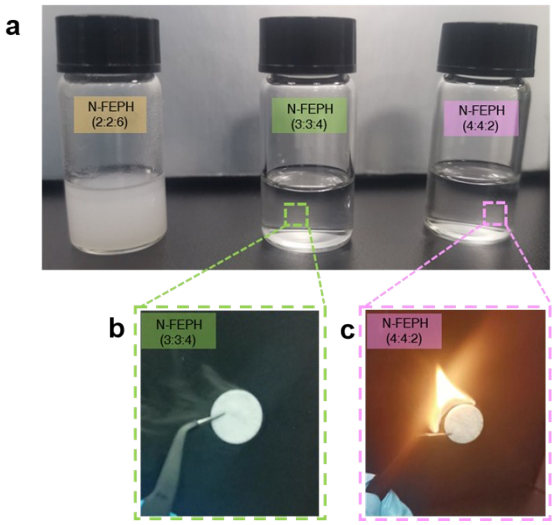

Figure S4. (**a**) Optical photos of the 1.0 M $NaPF_6$ in FEC/PC/HFE (N-FEPH) with the ratio of FEC/PC/HFE to be 2:2:6; 3:3:4 and 4:4:2 by vol%. Flammability tests of (**b**) N-FEPH (3:3:4) and (**c**) N-FEPH (4:4:2). By taming the compositing ratios while keeping FEC/PC ratio to 1:1, the electrolyte of N-FEPH (3:3:4) shows both intrinsic non-flammability and good salt solubility, which gives a clear solution. Turbidity is observed with the N-FEPH (2:2:6) electrolyte. We believe the strong Na^+-PF_6 interaction in the concentrated N-FEP (2:2) electrolyte is responsible. As reported by a recent work,[1] these highly-fluorinated ethers can further enhance the association between cations and anions, which is likely one reason contributing to salt precipitation and thus the electrolyte turbidity observed. Moreover, HFE molecules are reported to have poor affinity to the concentrated complexation in N-FEP (2:2), as stems from its relatively low dielectric constant and poor salt solubility,[2] further yielding the immiscibility with N-FEP (2:2) and causing the turbidity. Thus, we lowered the ratio of HFE and found that N-FEPH (3:3:4) and N-FEPH (4:4:2) electrolytes are clear.

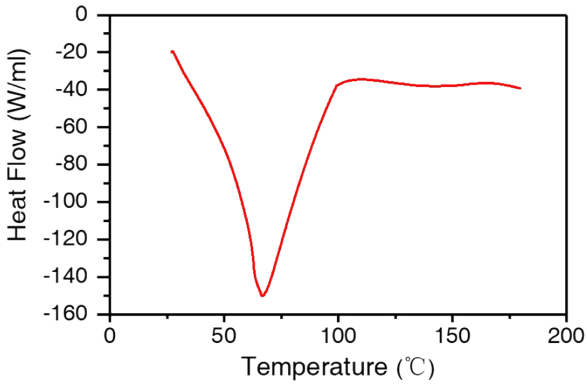

Figure S5. DSC curve of the PFMP fire extinguishant. A sharp endothermic peak is located at ~60°C, which helps to dissipate the generated heat *in-situ*.

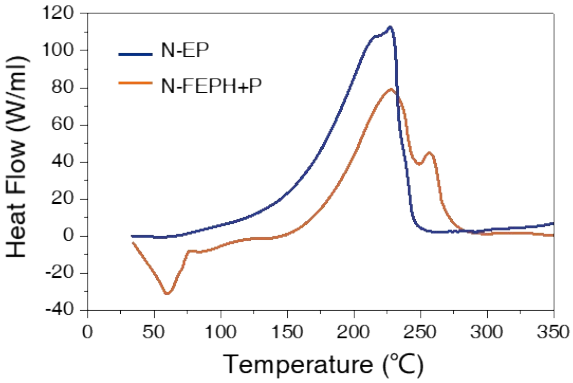

Figure S6. DSC curve of the N-EP and N-FEPH+P electrolyte. The conventional N-EP electrolyte shows strong exothermic peak at ~210-230°C. When PFMP is added to the electrolyte, the N-FEPH+P electrolyte exhibits an obvious endothermic peak in the lower temperature range, proving a self-cooling effect. As the temperature increases, two endothermic peaks appear at 227°C and 256°C, giving less heat release compared to the N-EP electrolyte.

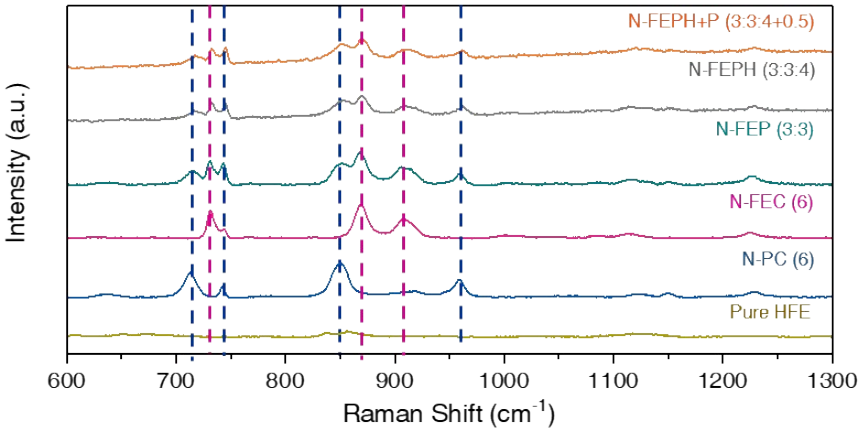

Figure S7. Raman spectra of the corresponding electrolyte systems. Here, the volume of salt-dissolving solvents (namely the FEC and PC) has been fixed at 6 shares, which aims to exclude the interference of peak shifting induced by different salt concentrations.

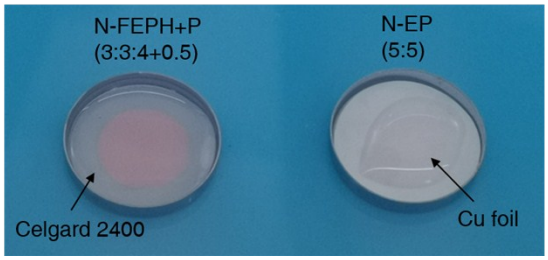

Figure S8. Wettability tests of the N-EP and N-FEPH+P electrolytes.

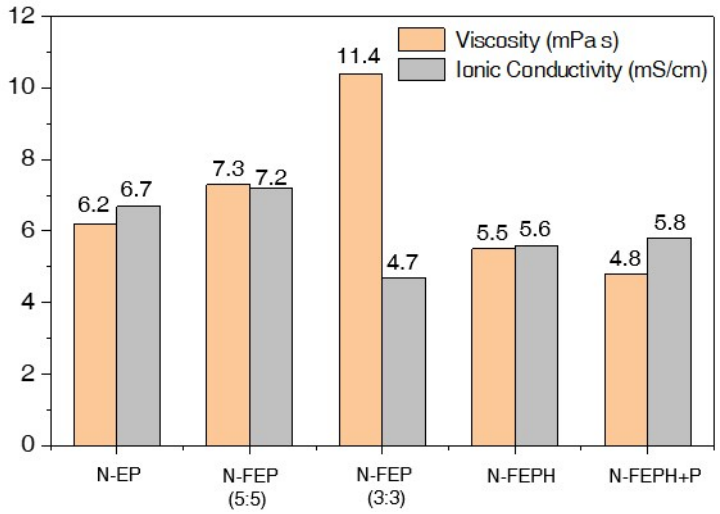

Figure S9. Viscosity and ionic conductivity of the corresponding electrolytes at room temperature. Here the N-FEP (3:3) refers to a volume of 6 shares and N-FEP (5:5) manifests a total of 10 shares, these two electrolytes exhibit same amount of $NaPF_6$ salt, which is 1.0*(5/3) M for N-FEP (3:3) and 1.0 M for N-FEP (5:5). After diluting N-FEP (3:3) with 4 shares of HFE, the resultant electrolyte of N-FEPH demonstrates a salt concentration of 1.0 M.

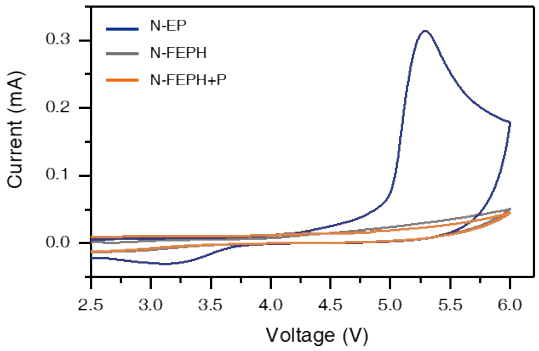

Figure S10. Cycling voltammetry (CV) curve of the corresponding electrolytes at a scan rate of 5 mV/s.

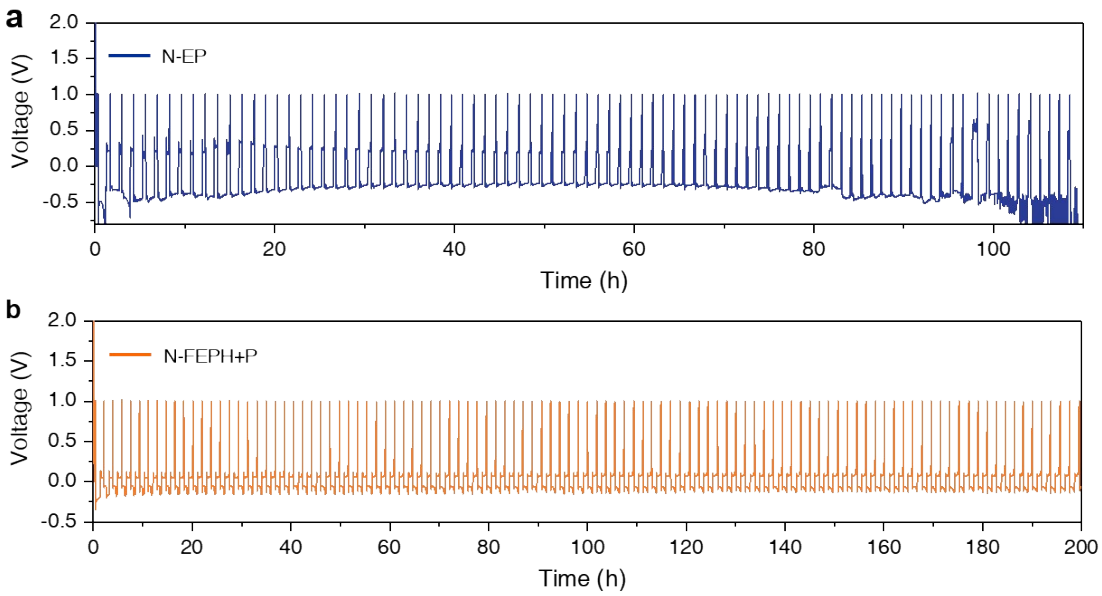

Figure S11. Voltage-time profiles of Na plating/stripping in the electrolyte of (**a**) N-EP and (**b**) N-FEPH+P at 0.5 mA/cm^2, 0.5 mAh/cm^2 for 100 cycles. Severe voltage oscillations can be observed when cycling in N-EP electrolyte, whereas the cell based on N-FEPH+P electrolyte exhibited very stable voltage profiles.

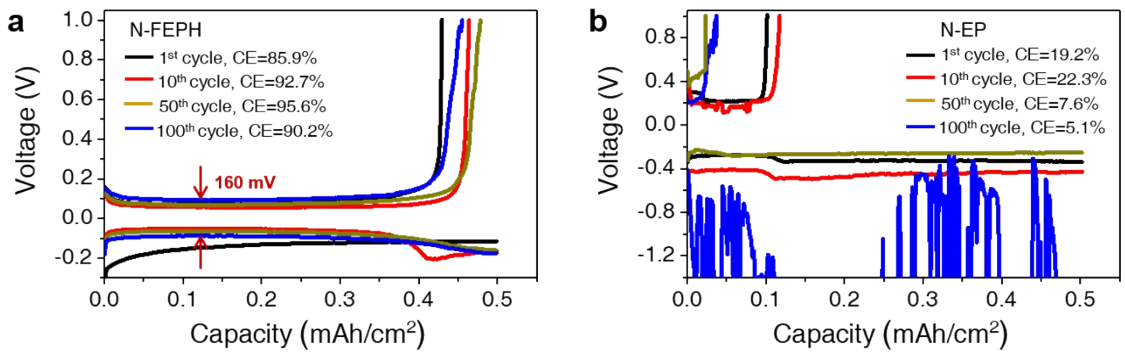

Figure S12. Voltage profiles for the Na/Cu cell at the 1st, 10th, 50th and 100th cycle with the electrolyte of (**a**) N-FEPH and (**b**) N-EP at 0.5 mA/cm^2, 0.5 mAh/cm^2.

It can be seen that the Na/Cu cell polarization with N-FEPH electrolyte remains almost constant, which has been restricted within 160 mV after 100 cycles. Whereas the N-EP-based counterpart manifests an initial polarization of 530 mV at the 1st cycle, with violently fluctuated voltage profiles seen at the 100th cycle.

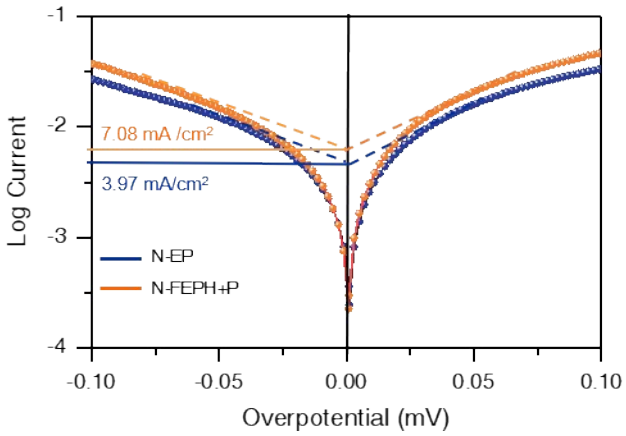

Figure S13. Tafel plots for Na plating/stripping in the electrolyte of N-EP and N-FEPH+P. The plot was obtained by fitting a small overpotential region from the cyclic voltammetry curve of the Na/Na symmetrical cells at 2 mV/s to the Tafel equation: $\eta=a+b\lg I$, where I, η represents the current and overpotential, respectively; a, b stands for a constant, as can be aquired after fitting the data. When overpotential of $\eta=0$, $\lg I_0$ can be obtained from the intercept with the vertical axis.[3]

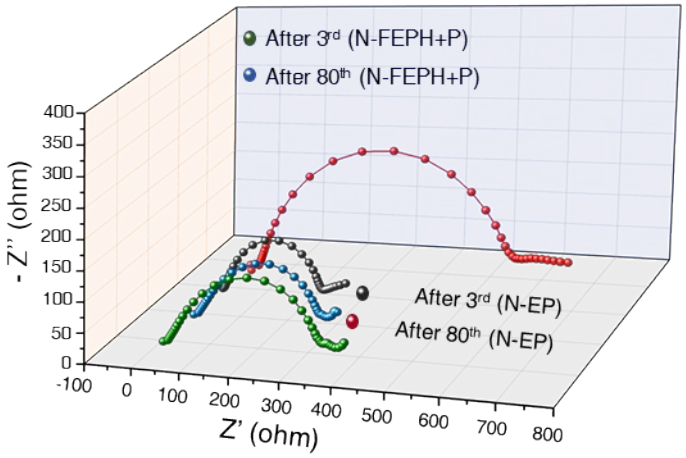

Figure S14. Nyquist plot of the Na/Na symmetrical cells using N-EP and N-FEPH+P electrolytes after cycling for 3rd and 80th cycles at 0.5 mA/cm^2, 1.0 mAh/cm^2.

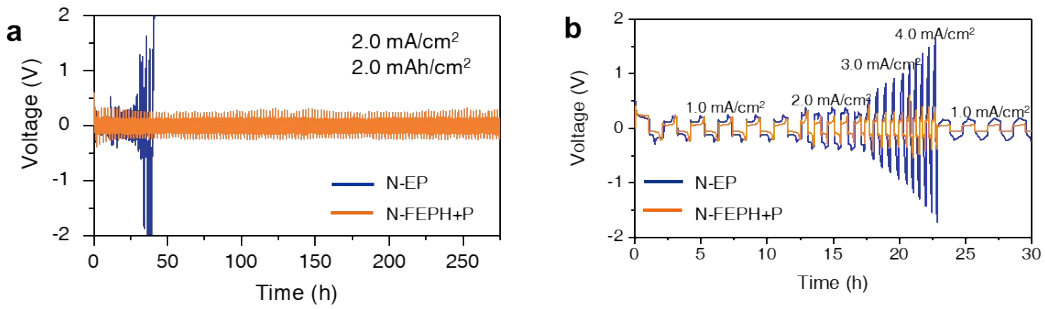

Figure S15. (**a**) Galvanostatic plating/stripping of the Na/Na symmetrical cells in N-EP and N-FEPH+P electrolytes at 2.0 mA/cm^2, 2.0 mAh/cm^2. (**b**) Rate behavior of the Na/Na symmetrical cells in N-EP and N-FEPH+P electrolytes at current densities of 1.0 mA/cm^2, 2.0 mA/cm^2, 3.0 mA/cm^2, 4.0 mA/cm^2 with a fixed capacity of 1.0 mAh/cm^2.

By increasing the plating/stripping current density and capacity to 2.0 mA/cm^2 and 2.0 mAh/cm^2, respectively. The control cell experienced fast voltage spiking, while long-term stability over 250 h is attained with N-FEPH+P electrolyte. When cycling under mutative current densities from 1.0 to 4.0 mA/cm^2, the Na metal electrode in N-FEPH+P operates stably with steadily growing voltage plateaus, whereas the overpotential using N-EP is evidently higher and increases fast with time.

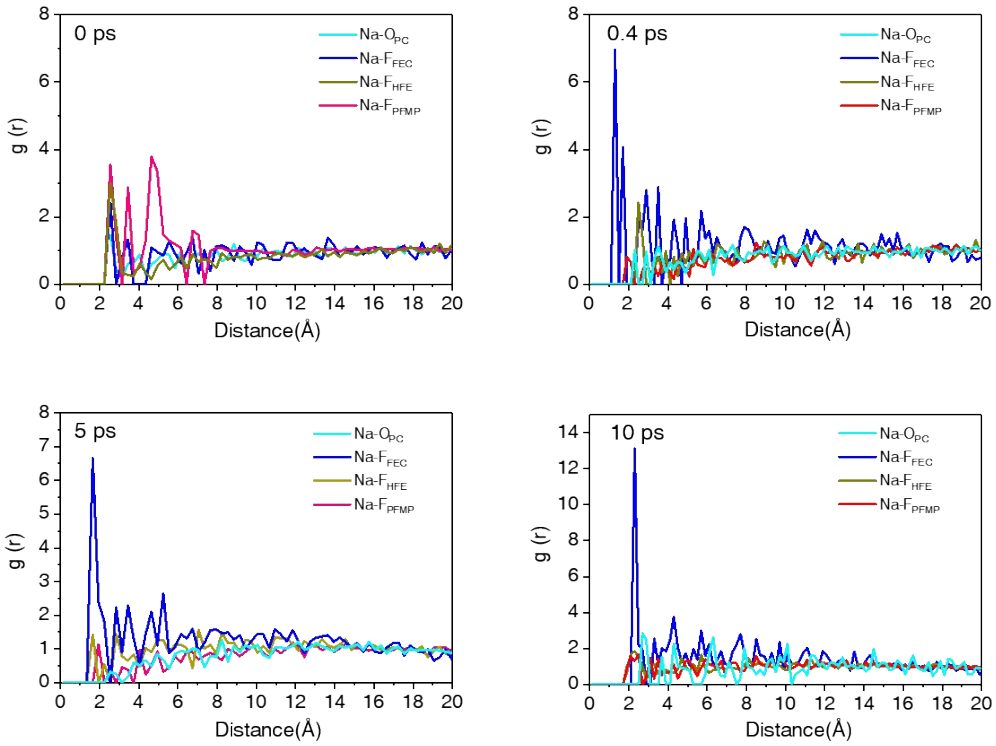

Figure S16. Radial distribution functions g(r) of Na-F_{FEC}, Na-F_{HFE}, Na-F_{PFMP}, and Na-O_{PC} calculated from AIMD calculations at 0 ps, 0.4 ps, 5 ps and 10 ps.

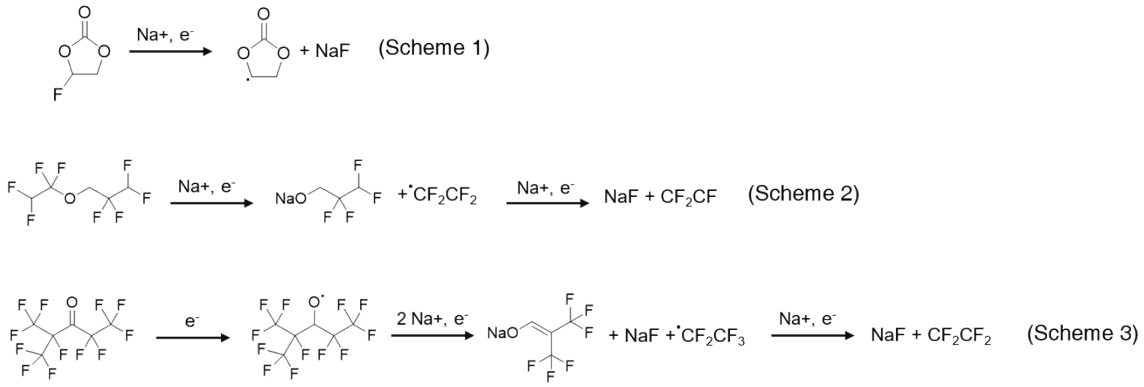

Scheme S1-S3. Proposed defluorination mechanisms of FEC, HFE and PFMP on Na metal anode.

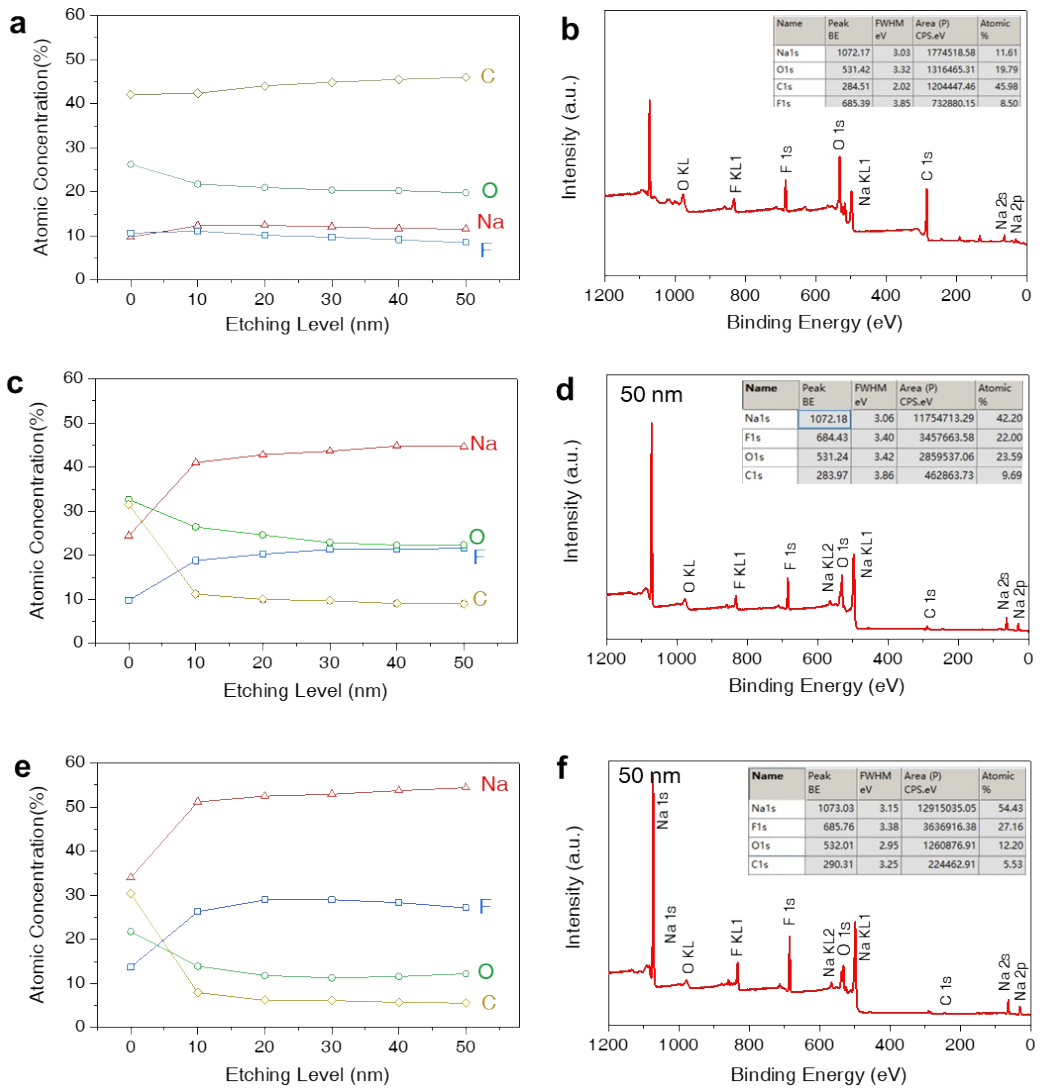

Figure S17. Atomic ratios of the C 1s, O 1s, Na 1s and F 1s on the Na metal at various durations of Ar^+ sputtering in (**a**) N-EP, (**c**) N-FEPH and (**e**) N-FEPH+P electrolytes after 80 cycles. XPS full survey spectra on the Na metal at a sputter depth of 50 nm in (**b**) N-EP, (**d**) N-FEPH and (**f**) N-FEPH+P electrolytes after 80 cycles.

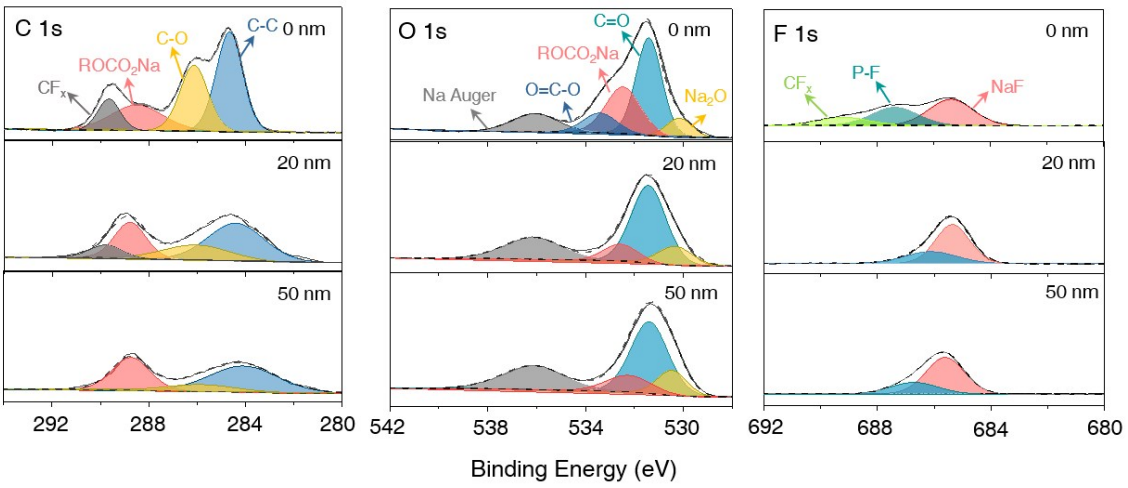

Figure S18. C 1s, O 1s and F 1s XPS depth profiles of the Na metal electrode after 80 cycles in N-EP electrolyte.

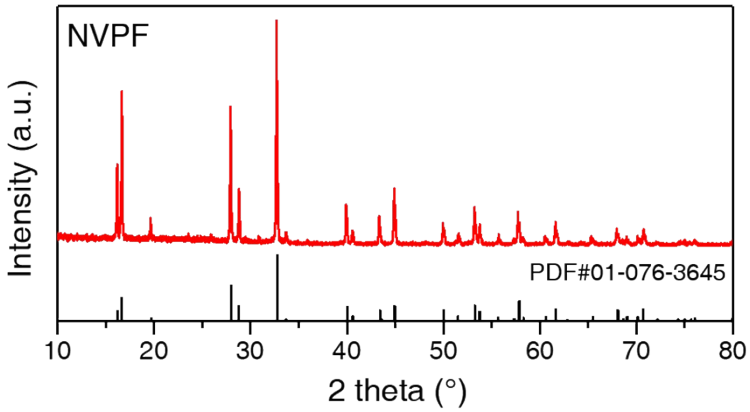

Figure S19. XRD pattern of the as-synthesized NVPF material.

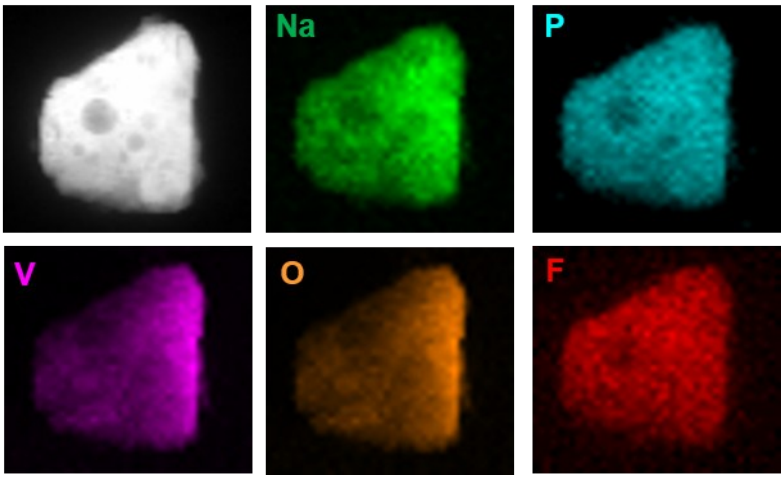

Figure S20. The HADDF-STEM image of the NVPF cathode with its corresponding elemental mapping of Na, P, V, O, and F. The uniform elemental distribution can be seen.

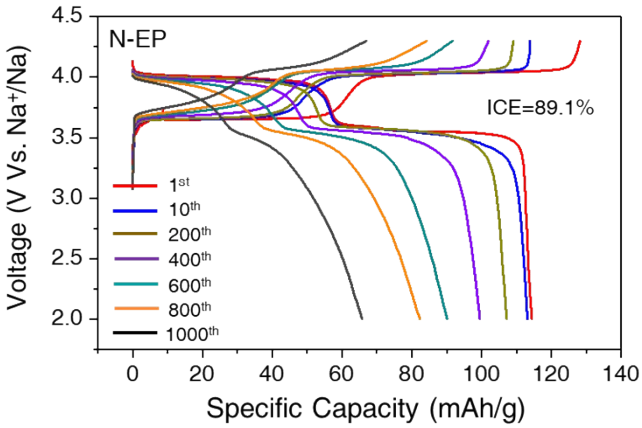

Figure S21. Voltage profiles of the Na/NVPF cells using N-EP electrolyte at the 1st, 10th 200th, 400th, 600th, 800th, 1000th cycle.

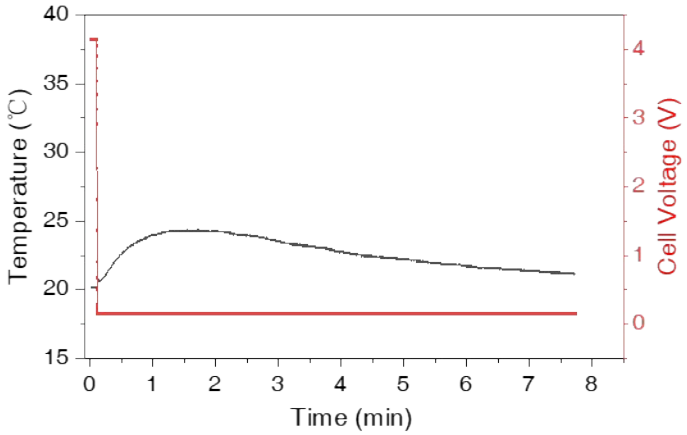

Figure S22. Nail penetration test on the Na/NVPF punch cell with the N-FEPH+P electrolyte. The cell temperature started to rise as soon as the cell was short-circuited upon nail penetration, however, the temperature rise was minor.

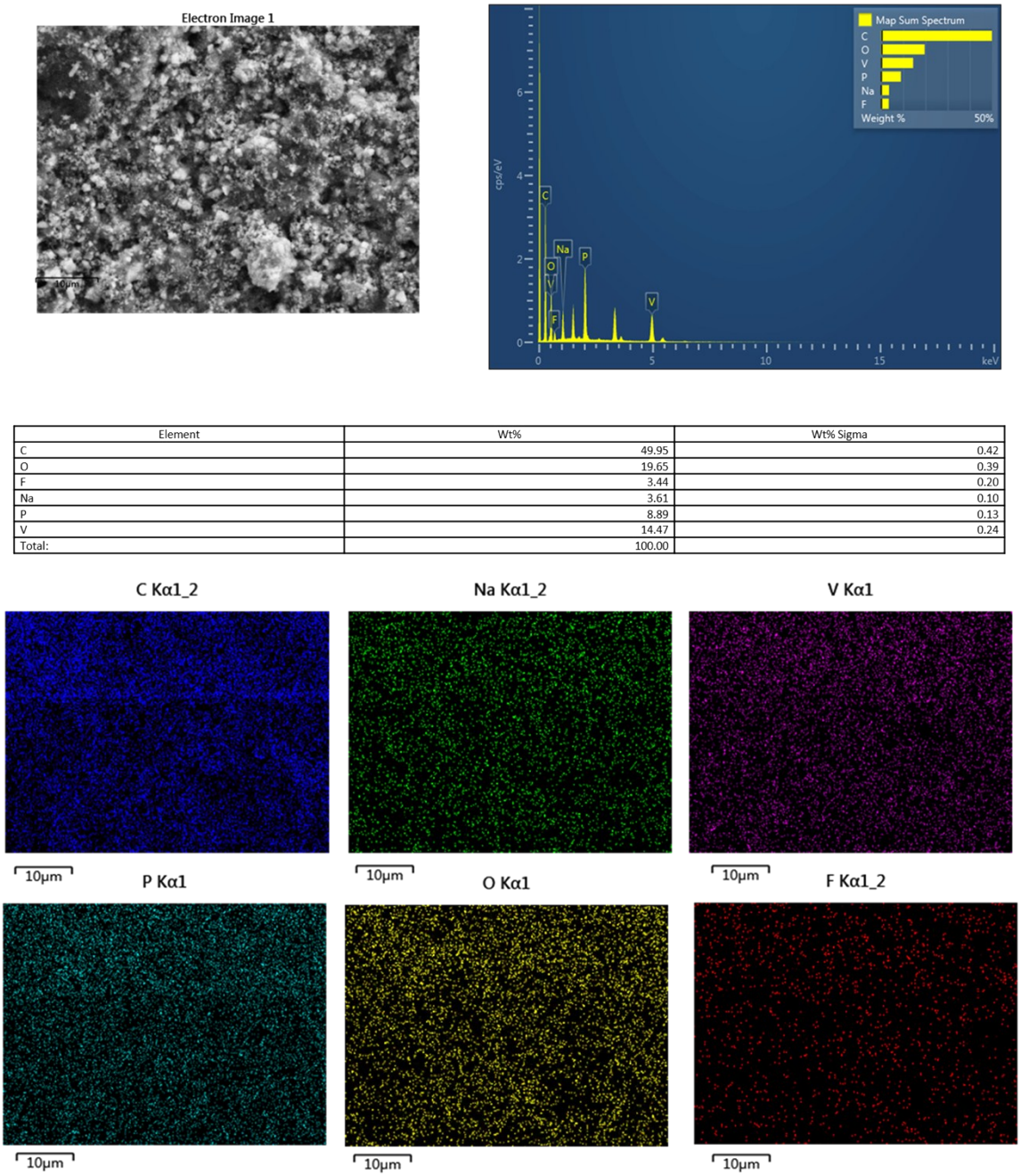

Element	Wt%	Wt% Sigma
C	49.95	0.42
O	19.65	0.39
F	3.44	0.20
Na	3.61	0.10
P	8.89	0.13
V	14.47	0.24
Total:	100.00	

Figure S23. EDX spectra and EDX elemental mapping of the the NVPF cathode after 80 cycles in N-EP electrolyte. The cycled electrode manifests pervasive cracks with ambiguous particles, showing the complete coverage by CEI. The lower F concentration also indicates the CEI with less F-content.

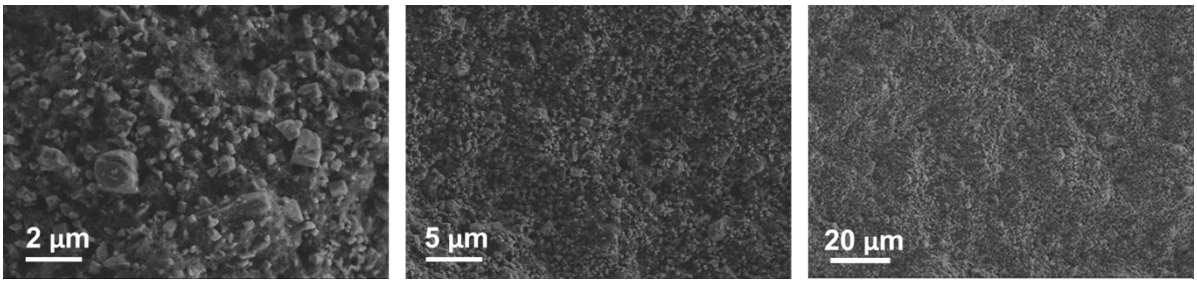

Figure S24. The SEM images of the pristine NVPF cathode at different magnifications. The edges of the particles can be clearly observed.

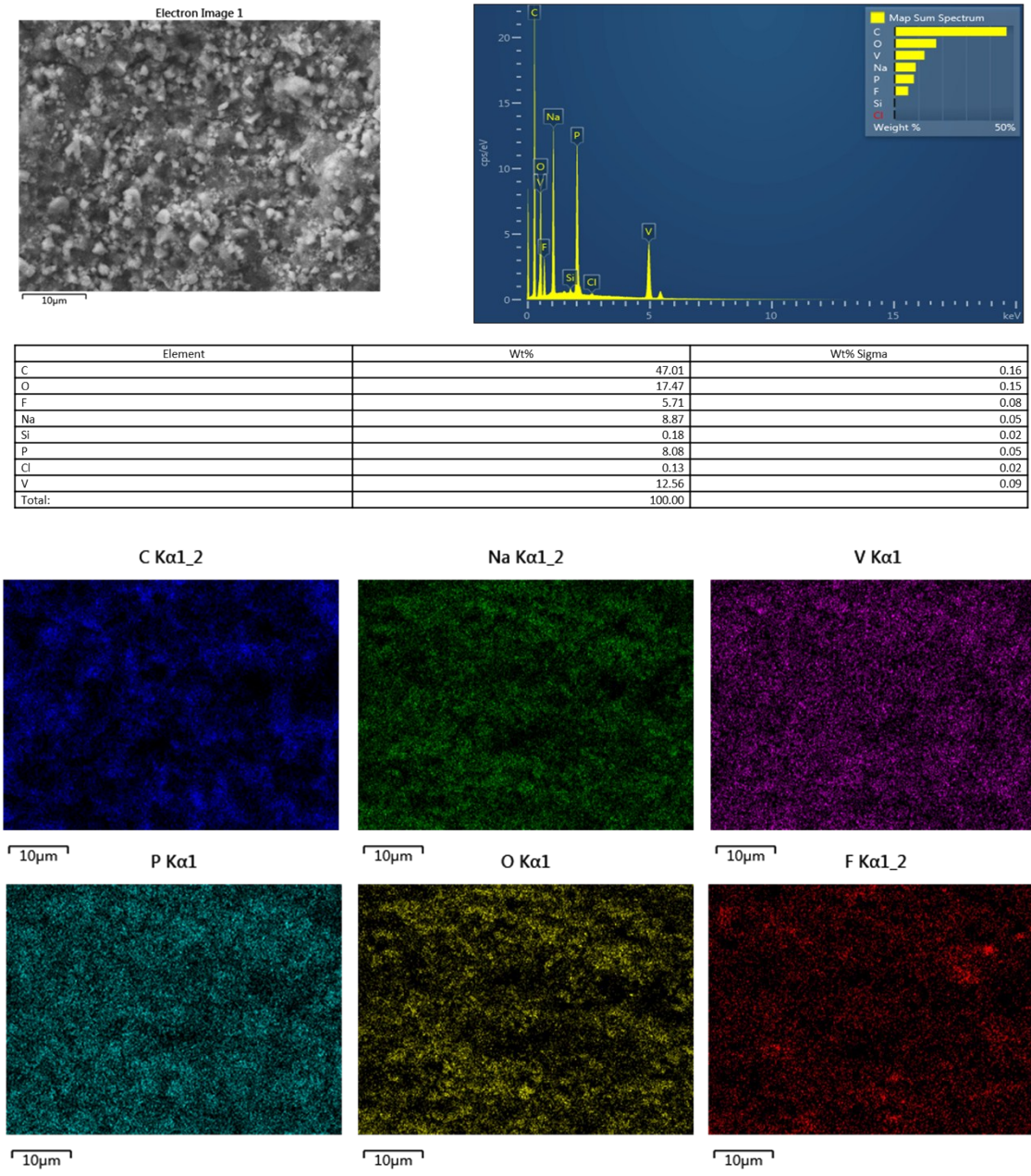

Element	Wt%	Wt% Sigma
C	47.01	0.16
O	17.47	0.15
F	5.71	0.08
Na	8.87	0.05
Si	0.18	0.02
P	8.08	0.05
Cl	0.13	0.02
V	12.56	0.09
Total:	100.00	

Figure S25. EDX spectra and EDX elemental mapping of the the NVPF cathode after 80 cycles in N-FEPH+P electrolyte. The edges of the active particles can still be seen. The electrode also shows higher concentration F element.

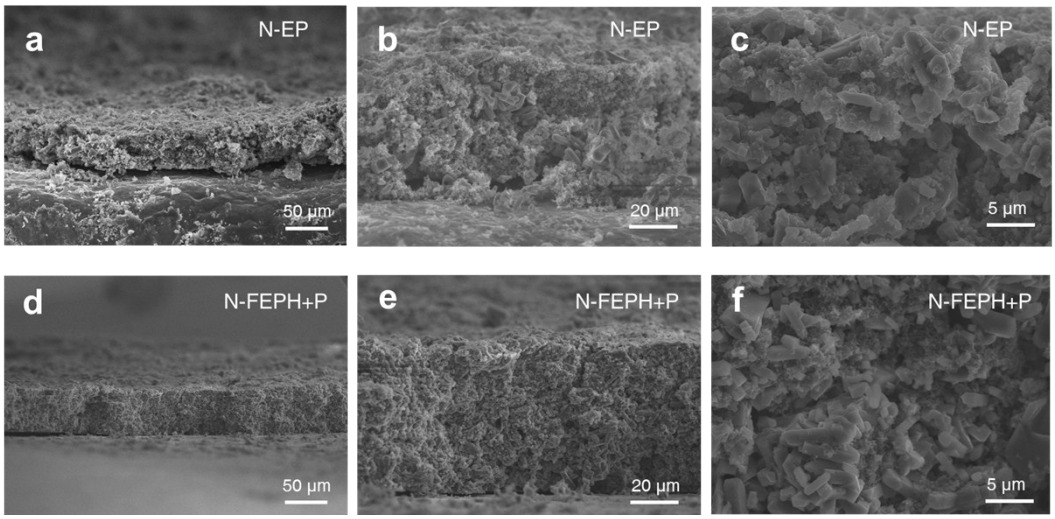

Figure S26. Cross-sectional SEM images of the NVPF cathode after 80 cycles in (a-c) N-EP or (d-f) N-FEPH+P electrolyte at different magnifications.

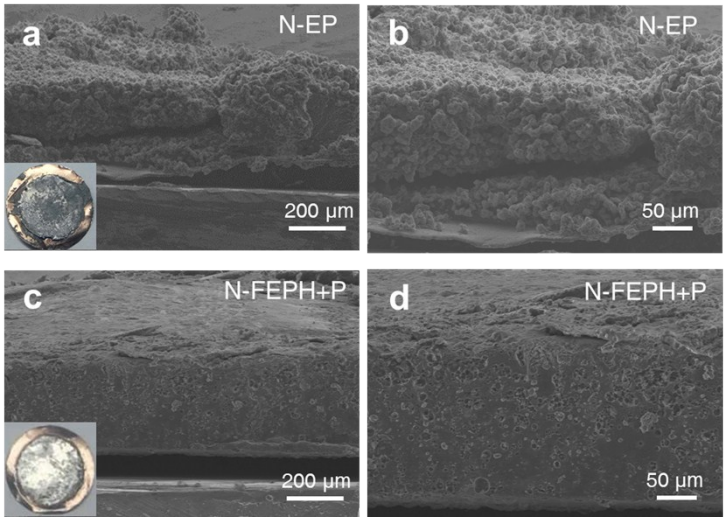

Figure S27. Cross-sectional SEM images of the Na metal anode after 80 cycles in (a,b) N-EP or (c,d) N-FEPH+P electrolyte at different magnifications.

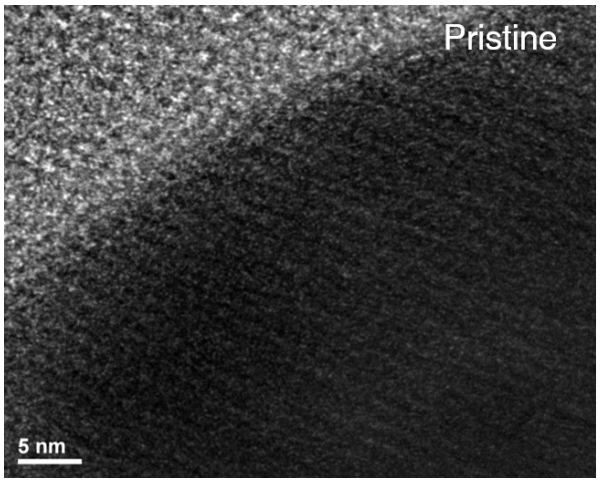

Figure S28. HRTEM image of the pristine NVPF particles.

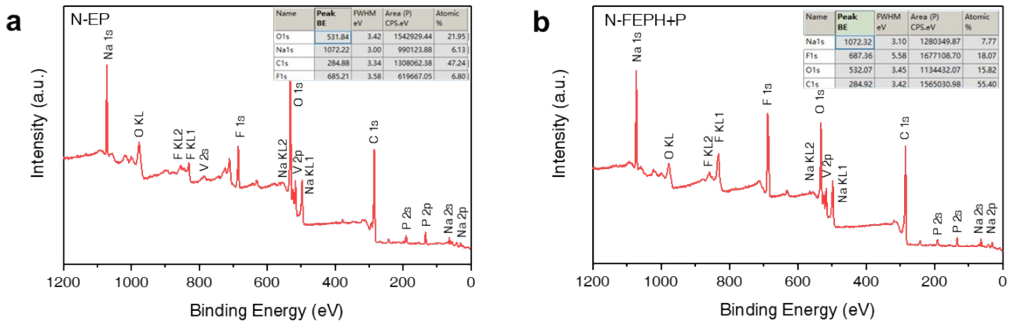

Figure S29. XPS full survey spectra on the NVPF cathode in (**a**) N-EP and (**b**) N-FEPH+P electrolytes after 80 cycles.

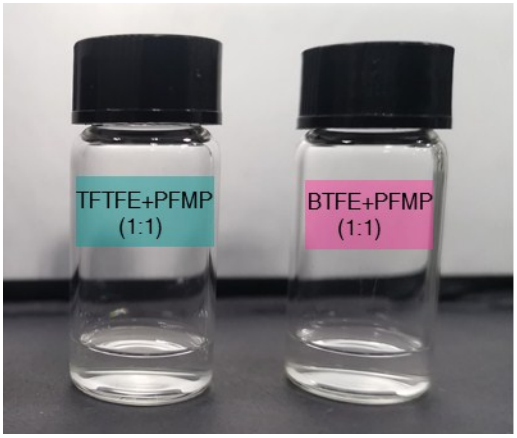

Figure S30. Optical photo showing the complete miscibility of TFTFE and BTFE with PFMP, with a volumetric ratio of 1:1 vol%. Here, their miscibility with both the electrolyte and PFMF endows them as effective bridge solvent to enable the miscibility of PFMP into conventional electrolyte.

Supplementary References

1. N. Piao, X. Ji, H. Xu, X. Fan, L. Chen, S. Liu, M. N. Garaga, S. G. Greenbaum, L. Wang, C. Wang and X. He, *Adv. Energy Mater.*, 2020, **10**, 1903568.
2. X. Ren, S. Chen, H. Lee, D. Mei, M. H. Engelhard, S. D. Burton, W. Zhao, J. Zheng, Q. Li, M. S. Ding, M. Schroeder, J. Alvarado, K. Xu, Y. S. Meng, J. Liu, J.-G. Zhang and W. Xu, *Chem*, 2018, **4**, 1877-1892.
3. Z. Tu, S. Choudhury, M. J. Zachman, S. Wei, K. Zhang, L. F. Kourkoutis and L. A. Archer, *Nat. Energy*, 2018, **3**, 310-316.